# Synthesis and Transformation of Linear Adamantane Assemblies inside Carbon Nanotubes

**Jinying Zhang,[†] Yanquan Feng,[‡,#] Hitoshi Ishiwata,[§] Yasumitsu Miyata,[†] Ryo Kitaura,[†] Jeremy E. P. Dahl,[§] Robert M. K. Carlson,[§] Hisanori Shinohara,[†,*] and David Tománek[‡,*]**

[†]Department of Chemistry and Institute for Advanced Research, Nagoya University, Nagoya, 464-8602, Japan, [‡]Department of Physics and Astronomy, Michigan State University, East Lansing, Michigan 48824-2320, United States, [§]Stanford Institute for Materials and Energy Science, Stanford University, Stanford, California 94305, United States, and [#]School of Physics, Beijing Institute of Technology, Beijing 100081, People's Republic of China

**ABSTRACT**

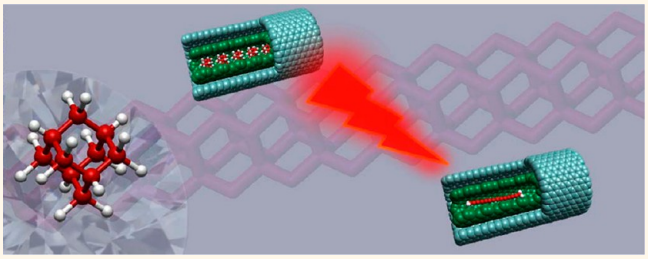

We report the assembly and thermal transformation of linear diamondoid assemblies inside carbon nanotubes. Our calculations and observations indicate that these molecules undergo selective reactions within the narrow confining space of a carbon nanotube. Upon vacuum annealing of adamantane molecules encapsulated in a carbon nanotube, we observe a sharp Raman feature at 1857 $cm^{-1}$, which we interpret as a stretching mode of carbon chains formed by thermal conversion of adamantane inside a carbon nanotube. Introduction of pure hydrogen during thermal annealing, however, suppresses the formation of carbon chains and seems to keep adamantane intact.

**KEYWORDS:** one-dimensional diamondoid derivative nanostructure · linear adamantane assembly · diamondoid · carbon chain · DWCNTs · nanotube confinement

Diamondoids are $sp^3$-hybridized carbon-based molecules containing cubic-diamond crystal-cages and surfaces terminated by hydrogen. They are structurally rigid, display high thermodynamic stability, yet can be chemically functionalized[1,2] to produce a wide-variety of useful materials, notably pharmaceuticals and high temperature polymers. Diamondoids have large band gaps[3] and exhibit excellent thermal conductivity.[2,4] The chemistry of diamondoids has recently been reviewed by Schwertfeger *et al.*[2] Functionalized diamondoids have played an important role as antiviral drugs for many years and have been used in the treatment of Alzheimer's disease.[2,5,6] Diamondoid derivative nanostructures and higher diamondoids have a variety of nanometer-sized geometric shapes[7] that determine their optical response.[8] Diamondoids fit into nanotubes[3] and show many interesting and useful properties including electron emission[9,10] and low-kappa dielectric response,[11] making them of great interest for nanotechnological and other applications.

A relatively simple and convenient way to form linear arrays of diamondoid molecules is by self-assembly within the confining space of a carbon nanotube, which determines the relative orientation and interaction between adjacent diamondoid molecules. However, the characterization of diamondoids encapsulated in nanotubes is extremely difficult due to the small molecule size that displays only $sp^3$ hybridization of carbon and hydrogen atoms.[12] A linear diamondoid assembly enclosed inside a carbon nanotube is a new one-dimensional $sp^3$ carbon nanostructure that combines properties of diamondoids and carbon nanotubes and thus has promising applications in electronic and optical nanotechnology.[8−11] The narrow cavity of the enclosing carbon nanotube also provides an excellent constraint for directing further reactions toward shape-targeted nanostructures. In analogy to the formation of $sp^2$ hybridized carbon nanostructures by fusing zero-dimensional nanostructures (fullerenes) to one-dimensional assemblies (nanotubes),[13−17] we consider the possibility that also zero-dimensional $sp^3$ hybridized carbon nanostructures (diamondoids) may aggregate and transform to one-dimensional $sp^3$ hybridized carbon structures, which we call diamond nanowires.

Templated growth of $sp^3$ carbon nanostructures from diamondoids confined

* Address correspondence to noris@nagoya-u.ac.jp, tomanek@pa.msu.edu.

Received for review May 19, 2012 and accepted August 24, 2012.

**Published online August 24, 2012**
**10.1021/nn303461q**

within narrow carbon nanotubes would be a completely new way to synthesize diamond nanowires and higher diamondoids. Adamantane ($C_{10}H_{16}$), the smallest diamondoid, is readily synthesized using superacid catalysts by a method developed by Schleyer.[18] Successive members of the diamondoid series contain an additional adamantane-cage "face-fused" to its next lower member. Diamondoids with more than three cages (tetramantanes, pentamantanes, *etc.*) cannot be synthesized using superacid catalysts, but were recently isolated from petroleum.[7] Each higher diamondoid has several structural forms as additional cages can add to various faces, which gave rise to a higher diamondoid nomenclature developed by Balaban and Schleyer.[19] Inside a compatible carbon nanotube the only possible direction for diamond cage addition is the preferred end-on addition that provides the desired molecular orientation.

In this work, we report theoretical and experimental studies of the synthesis and transformation of one-dimensional diamondoid derivative nanostructures, including linear adamantane assemblies, in the confining space of a double-wall carbon nanotube (DWCNT). Our calculations indicate that adamantane molecules favor encapsulation inside selective carbon nanotubes, but do not react spontaneously even at high temperatures. The predicted encapsulation has been achieved using high temperature sublimation of adamantane molecules that filled open-ended DWCNTs, as described in the Methods section. The as-synthesized linear adamantane assemblies inside DWCNTs (ad@DWCNTs) were annealed and subsequently underwent a transformation, depending on the specific annealing conditions. The $sp^3$ hybridized nanostructures were found to convert into carbon chains inside a carbon nanotube when annealed in vacuum at temperatures above 500 °C. We found the as-produced carbon chains, which were spectroscopically characterized by a sharp Raman feature at 1857 $cm^{-1}$ originating from a C−C stretching mode, to be stable inside carbon nanotubes with inner diameters around 1.0 nm. Nanotubes with an inner diameter exceeding 1.3 nm were found to often contain multiple chains, which seemed to react with defects of the wall and possibly even to escape from the inner space under electron beam irradiation. Introduction of pure hydrogen during thermal annealing, however, suppressed the formation of carbon chains and kept adamantane intact.

## RESULTS AND DISCUSSION

The low sublimation and high decomposition temperature of adamantane[20] are favorable prerequisites for the assembly and transformation of linear adamantane assemblies within the confinement space of a carbon nanotube from vapor phase, as described in Scheme 1. Further transformation of the as-produced linear adamantane assemblies into different structures

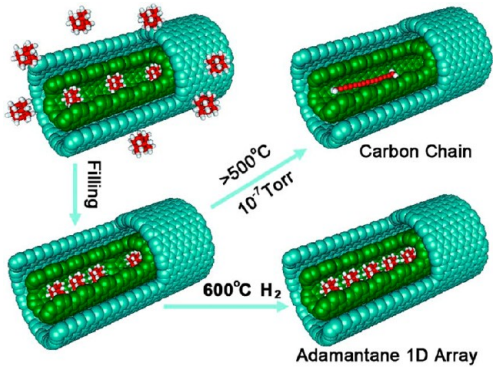


**Scheme 1. Synthesis and Annealing of Linear Adamantane Assemblies**

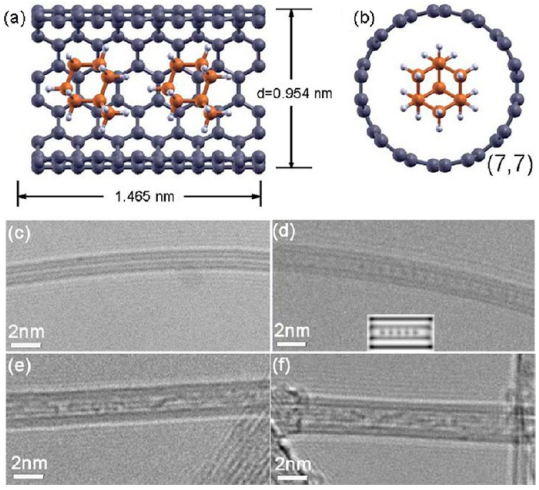


**Figure 1. Optimized equilibrium structure of two adamantane molecules inside a (7,7) carbon nanotube in (a) side and (b) end-on view. HR-TEM images of adamantane molecules encapsulated in DWCNTs with inner diameter (c) $d < 0.8$ nm (no encapsulation), (d) $d \approx 1.0$ nm (single linear array of adamantane molecules), (e) $d \approx 1.4$ nm (double array of adamantane molecules), (f) $d \approx 1.8$ nm (multiple arrays of adamantane molecules).**

was observed following annealing at different temperatures and in different atmospheres.

As suggested by early theoretical results,[3] we found the encapsulation of adamantane in carbon nanotubes to be highly diameter selective. The adamantane structure inside a (7,7) carbon nanotube at $T = 0$ K, depicted in Figure 1a,b, maximizes the attractive adamantane−nanotube interaction. As seen in Figure 1a, the adamantane molecules prefer to stay at the center of the carbon nanotube cavity on energetic grounds and are about at van der Waals distance from the enclosing nanotube walls. The net energy gain of 0.88 eV per adamantane molecule upon encapsulation is responsible for an efficient filling of the nanotubes. This energy gain is caused to a large degree by the hybridization of adamantane states with those of the enclosing nanotube, causing minor changes in the electronic structure. We found the energy gain to be smaller in wider nanotubes, where this hybridization is

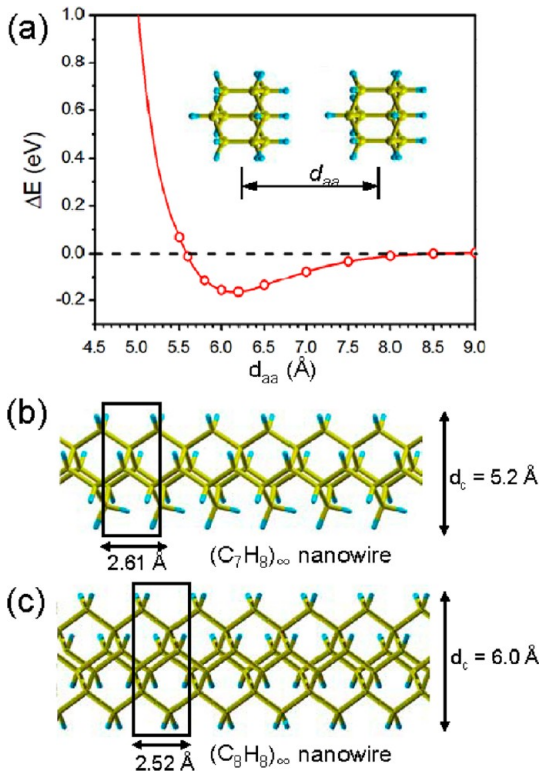


**Figure 2. Equilibrium structure of linear arrays of adamantane molecules and candidate structures for diamond nanowires that may form inside narrow carbon nanotubes. (a) Interaction between adjacent adamantane molecules as a function of their separation $d_{aa}$. The equilibrium geometry of a postulated $(C_7H_8)_\infty$ (b) and a $(C_8H_8)_\infty$ (c) diamond nanowire that may fit inside a (7,7) nanotube.**

smaller, and the filling process to be endothermic in narrow nanotubes[3] with diameters $d < 0.8$ nm. Once inside a nanotube, adjacent adamantane molecules assemble to a linear array with a preferential interadamantane distance $d_{aa} \approx 6.2$ Å, as seen in Figure 2a. The pairwise interadamantane interaction is weakly attractive, yielding only ~0.16 eV binding energy. A substantial repulsion occurs at shorter separations, consistent with the fact that adamantane molecules are rather unreactive.

Our HR-TEM observations agree well with the above predictions, since no encapsulated adamantane in DWCNTs with inner diameters below 0.8 nm was detected (Figure 1c). Single linear arrays of adamantane molecules were only detected in DWCNTs with inner diameters around 1 nm (Figure 1d). Our observations were found to be consistent with simulated TEM images of carbon chains inside a nanotube (inset of Figure 1d). Two and three linear arrays of adamantane molecules were detected in nanotubes with diameters around 1.4 nm (Figure 1e) and 1.8 nm (Figure 1f), respectively.

Beside the stability of adamantane molecules inside carbon nanotubes, we also calculated vibration spectra of pristine adamantane, a pristine (7,7) carbon nanotube, adamantane inside the nanotube, and the postulated $(C_7H_8)_\infty$ and $(C_8H_8)_\infty$ diamond nanowire. These spectra were obtained from the velocity–velocity autocorrelation functions accumulated during MD simulations at $T \approx 1300$ °C and are presented in Figure 3a–d. We find that the spectrum of a nanotube containing adamantane molecules in Figure 3d differs significantly from the spectrum of the postulated diamond nanowires in Figure 3b. It resembles much more closely a superposition of the spectra of adamantane in Figure 3a and of the enclosing nanotube in Figure 3c. The vibration spectrum of adamantane in Figure 3a consists of C–C stretching modes in the frequency range up to ~1400 $cm^{-1}$ and of C–H stretching modes at 2800–2900 $cm^{-1}$, which had been previously discussed in computational studies of diamondoid molecule lattices.[29] As seen in Figure 3d, these modes persist, but are modified inside the nanotube.

The encapsulation of adamantane molecules into DWCNTs was also characterized by ATR-FTIR, as shown in Figure 3e. Our ATR-FTIR spectra, shown by the blue dashed line in Figure 3e, exhibit a carbon–hydrogen stretching vibration of $CH_2$ (6) at 2897 $cm^{-1}$ and CH (4) at 2845 $cm^{-1}$, in good agreement with our simulations in Figure 3d and published results.[21] Besides the adamantane molecules encapsulated inside the nanotubes during the vapor phase reaction, a large quantity of adamantane molecules condensed outside the nanotubes. The ATR-FTIR spectra of the sample at the completion of the filling process, shown by the red dotted line in Figure 3e, are dominated by the signal from adamantane molecules outside the carbon nanotubes. Since the spectrum of pure DWCNTs, shown by the black dash-dotted line in Figure 3e, is rather featureless, the spectrum of nanotubes exposed to adamantane is very similar to that of pure solid adamantane, given by the blue dashed line in Figure 3e.

Due to its high solubility in organic solvents[22] and low sublimation temperature,[20] molecules of adamantane outside DWCNTs were easily washed away by acetone and then sublimed in the oven at 90 °C overnight. Only encapsulated adamantane molecules remained in the sample following this procedure. This sample of DWCNTs containing encapsulated adamantane, ad@DWCNTs, was measured again by ATR-FTIR. Only carbon–hydrogen stretching vibrations of the encapsulated adamantane molecules were detected in the ATR-FTIR spectra, shown by the green solid line in Figure 3e. The major difference with respect to the spectrum of pure adamantane is a blue shift of the carbon–hydrogen stretching vibration frequency of $CH_2$ from 2897 to 2917 $cm^{-1}$ due to the confinement effects of DWCNTs, consistent with our theoretical results in Figure 3d. We did not observe any change in the frequency of the CH stretching mode at 2845 $cm^{-1}$. As mentioned earlier, the main objective of our study was to form 1D assemblies of adamantane

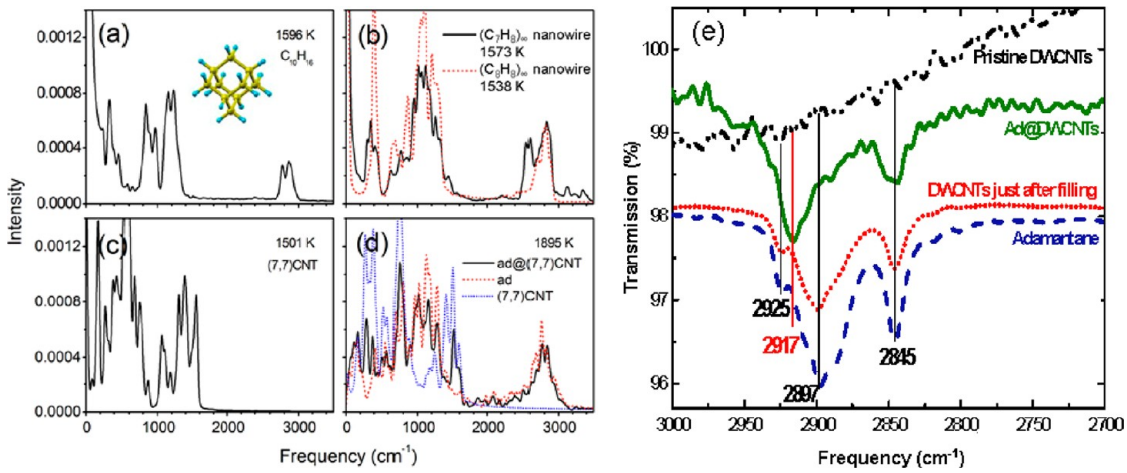


**Figure 3. Calculated high-temperature vibration spectrum of (a) an adamantane molecule, (b) postulated infinite $(C_7H_8)_\infty$ and $(C_8H_8)_\infty$ diamond nanowires, (c) an infinitely long (7,7) carbon nanotube, and of (d) this nanotube containing two adamantane molecules per $(C_{10}H_{16})_2@C_{168}$ unit cell. All vibration spectra, including the individual adamantane and nanotube components of the vibration spectrum in panel d, are normalized. (e) Experimental ATR-FTIR spectra of the transmission of DWCNTs at different stages of filling with adamantane. The different curves represent pristine DWCNTs (black dash−dotted line), pure adamantane (blue dashed line), adamantane both inside and outside of DWCNTs just after filling (red dotted line), and the ad@DWCNTs after removing of adamantane outside the nanotubes (green solid line).**

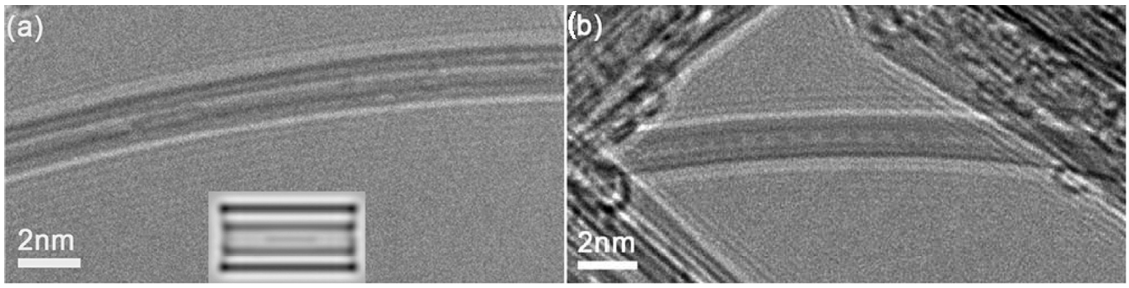


**Figure 4. (a) HR-TEM image of a sample that was annealed under $10^{-7}$ Torr vacuum, showing carbon chains inside the DWCNTs, which are also represented by the simulated TEM image in the inset. (b) HR-TEM image of the corresponding sample that was annealed under hydrogen atmosphere.**

and to explore the possibility of templated growth of higher diamondoids and diamond nanowires by means of transforming arrays of adamantane molecules within the constrained volume inside a carbon nanotube. Recently reported formation of higher from lower diamondoids,[23] albeit not selectively restricted to quasi-1D structural isomers, included the formation of the three tetramantanes,[7] [121], [(1(2)3], and [1234], from triamantane at pyrolytic temperatures of 500 °C. The study also showed that [1212] pentamantane, the 5-diamond-cage member of the linear, rod-shaped diamondoid series is the predominant product of pyrolytic treatment of the next lower member of that series, [121]tetramantane.[23] Figure 2c depicts the atomic structure of a candidate diamond nanowire structure. The ″rod″ shaped structural fragment, shown in Figure 2c, has 11 diamond cages and is a member of the linear diamond/diamondoid series, which also includes [121]tetramantane and [1212]pentamantane. The fragment structure has the Balaban−Schleyer[19] higher diamondoid name [-1212121212-]undecamantane. Formation of linear diamond structures, such as that in Figure 2c, *via* pyrolytic formation mechanism of higher diamondoids[23] appears possible, since linear, rod-shaped diamondoid precursors were found to aggregate preferentially end-on even in a macroscopic reaction vessel. Within the proposed templated growth mechanism,[23] which orients the molecules and suppresses nonlinear structures that do not fit inside a DWCNT, diamond nanowires $(C_7H_8)_\infty$ with diameters of 0.52 nm (Figure 2b) and $(C_8H_8)_\infty$ with diameter of 0.60 nm (Figure 2c) are the two most plausible structures if such diamond nanowires were to form by fusion of encapsulated adamantane molecules.

We annealed ad@DWCNTs at 600 °C under $10^{-7}$ Torr vacuum, similar to the conditions for fusing fullerenes from fullerene peapods,[17,24] and comparable to the pyrolytic temperature of diamondoids.[7] Under these conditions, we did not see large quantities of fused adamantane molecules, but rather observed linear carbon chains formed by conversion of adamantane. These carbon chains have been identified both by HR-TEM (see Figure 4a) and by Raman spectroscopy

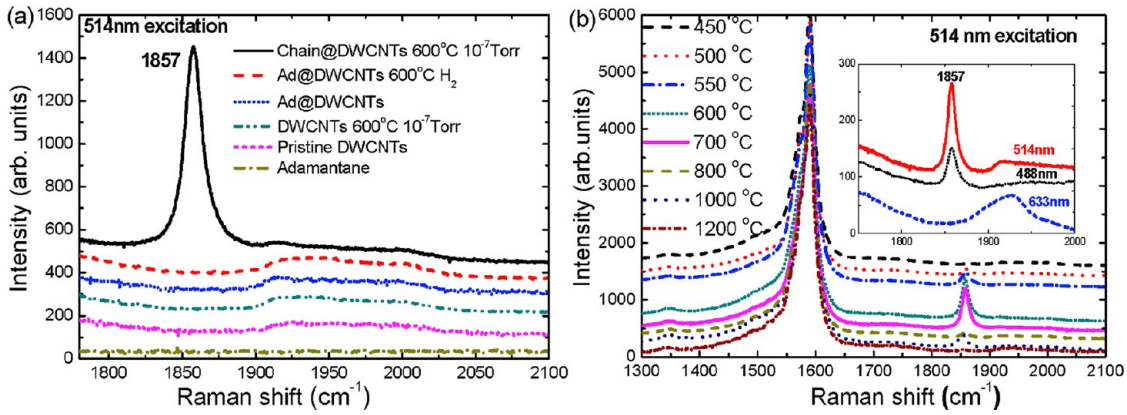


**Figure 5. (a) Raman spectra of pure adamantane, pristine DWCNTs, and DWCNTs filled with adamantane. Spectra of as-prepared samples at 300 °C are compared to samples annealed at 600 °C both in vacuum and in $H_2$ atmosphere. (b) Corresponding Raman spectra of ad@DWCNT samples annealed at different temperature under $10^{-7}$ Torr vacuum, observed using a laser wavelength $\lambda = 514$ nm under ambient conditions. Resonance spectra for different laser wavelengths are shown in the inset.**

(Figure 5). Our HR-TEM images allow us to clearly distinguish a carbon chain in Figure 4a from a linear array of adamantane molecules in Figure 1d. The observed and the simulated images of carbon chains, shown in the inset of Figure 4a, appear consistent with each other.

To spectroscopically characterize the system before and after high-temperature annealing, we compare Raman spectra of pure adamantane, pure DWCNTs, and DWCNTs exposed to different conditions in Figure 5a. Whereas most of these spectra are rather featureless in the frequency range 1800−2000 $cm^{-1}$, we observe a new feature at 1857 $cm^{-1}$ in the ad@DWCNTs sample that was annealed at 600 °C under a vacuum of $10^{-7}$ Torr, shown by the black solid line in Figure 5a. As suggested above, this Raman-active mode may be associated with carbon chains. We confirm that this spectral feature must be linked to adamantane encapsulation, since no feature at 1857 $cm^{-1}$ was observed in corresponding empty DWCNTs that were annealed under the same conditions.

There is a vast body of literature on both polyyne[25,26] and cumulene[27,28] allotropes and their Raman activity, which have been studied previously both theoretically and experimentally.[29−31] Raman spectral features from 1790 to 1860 $cm^{-1}$ have been observed and attributed to the vibration of one-dimensional carbon chains in multiwalled carbon nanotubes produced by direct current arc discharge[29,31] and high temperature annealing of DWCNTs (≈1600 °C).[32,33] Formation of polyynes has also been reported in the fusion products of $C_{10}H_2$ contained in carbon nanotubes.[30,34,35]

We also studied the conversion rate of ad@DWCNTs to carbon chains as a function of the annealing temperature and show our results in Figure 5b. The 1857 $cm^{-1}$ feature in the Raman spectra, associated with carbon chains, emerges as the ad@DWCNTs sample is annealed in vacuum to above 500 °C. The intensity of this Raman feature increases with increasing annealing temperature and reaches its maximum at temperatures between 600 and 700 °C, when the conversion of adamantane to carbon chains has been completed due to the lack of hydrogen to passivate $sp^3$ bonded carbons. Above 800 °C, the intensity of the 1857 $cm^{-1}$ feature starts decreasing again as the carbon chains start reacting and decomposing at high temperatures, in agreement with a recent study.[31] Our Raman spectra reported in Figure 5 were obtained using laser excitation energy of 2.54 eV ($\lambda$ = 488 nm), 2.41 eV ($\lambda$ = 514 nm), and 1.96 eV ($\lambda$ = 633 nm). As shown in the inset of Figure 5b, the Raman feature at 1857 $cm^{-1}$ was strongest under the $\lambda = 514$ nm excitation, and was nearly absent under the $\lambda = 633$ nm excitation.

We found that both the Raman feature frequency and its intensity dependence on the excitation energy were different in carbon chains produced from linear adamantane assemblies and in carbon chains obtained by conversion of encapsulated polyyne chains $C_{10}H_2$@DWCNTs.[30] Our Raman spectra suggest that carbon chains formed from linear ad@DWCNTs are much more uniform than those formed within arc discharge MWCNTs[29,31] or from enclosed polyyne chains $C_{10}H_2$@DWCNTs.[30] In particular, the sharp 1857 $cm^{-1}$ Raman feature was observed only in carbon chains formed by conversion of ad@DWCNTs.

The equilibrium structure of an infinitely long carbon chain is a linear arrangement of covalently bonded C atoms. The optimum geometry can be inferred by inspecting the total energy as a function of the alternating interatomic distances $r_1$ and $r_2$ in Figure 6a. The most stable structures are associated with a unit cell of constant length $r_1 + r_2 = 2.60$ Å. A very small stabilizing energy of 2 meV/$C_2$ causes a bond length change from $r_1 = r_2 = 1.30$ Å in the cumulene allotrope to what some call a polyyne allotrope with slightly different bond lengths. In reality, the bond length difference $r_1 - r_2 =$ 0.04 Å, which comes about due to a Peierls instability in

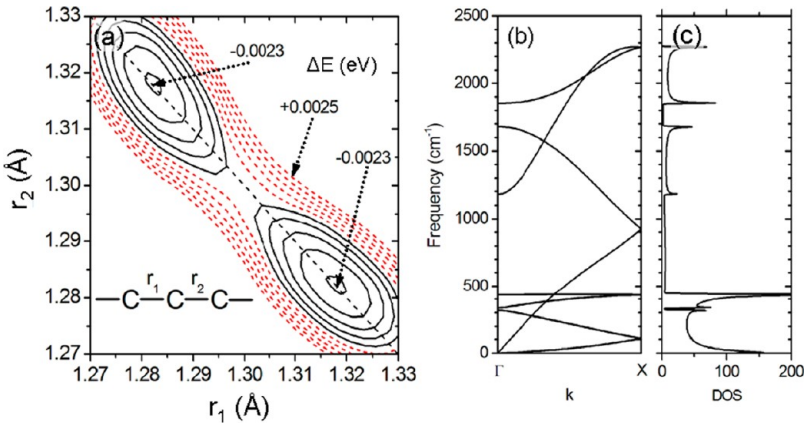


**Figure 6. (a) Total energy contour plot $\Delta E(r_1,r_2)$ of an infinite linear carbon chain with alternating interatomic distances $r_1$ and $r_2$, with $\Delta E$ presented per two-atom unit cell. The schematic in the inset addresses the geometry, not bonding character. (b) Vibrational band structure and (c) vibrational density of states (DOS) of a carbon chain.**

the electronic structure, is too small to clearly differentiate a triple from a single bond, so that the chain should most closely resemble a cumulene chain in its behavior.[27] The calculated vibrational band structure of the carbon chain is presented in Figure 6b and the corresponding density of states (DOS), dominated by characteristic van Hove singularities, in Figure 6c. We note that the observed new feature at 1857 $cm^{-1}$ in the Raman spectrum lies close to one of the van Hove singularities in the vibrational DOS shown in Figure 6c. We found that the chain binds only very weakly to the graphitic structure of the enclosing nanotube, with an equilibrium separation from the wall of 3.3 Å and a binding energy of only 0.04 eV per C atom of the chain. The weak coupling and physical closeness to the nanotube wall is expected to cause minor modifications in the vibration modes of the chain and the Raman selection rules.

Our *ab initio* calculations indicate that the formation of carbon chains involves more than a single-step thermal conversion of adamantane to elemental carbon and hydrogen, since the reaction

$$nC_{10}H_{16} \rightarrow 10nC\ (\text{chain}) + 8nH_2 - n\cdot\Delta E \qquad (1)$$

is a strongly endothermic process that requires a substantial amount of energy, $\Delta E = +20.8$ eV per adamantane molecule. Experimentally, we know that adamantane molecules start to decompose at temperatures above 660 °C into liquid pyrolyzates including benzenes and alkylbenzenes as well as unsaturated gaseous components including ethylene by breaking and reconnecting C−H and C−C bonds.[23,36] We observed that adamantane turns into black shiny structures, possibly consisting of graphitized carbon,[37] and a yellow oily suspension under vacuum conditions. Within the confining volume of a nanotube, realized in our experiment, we may observe emergence of other carbon structures, including sp hybridized carbon chains, as the end product under vacuum conditions.

Our HR-TEM observations at an electron current density of 20 pA/$cm^2$ (density at the detector at 300 K) indicate that the dynamics of as-produced carbon chains depends on the inner diameter of the enclosing DWCNT. Carbon chains contained in DWCNTs with an inner diameter around 1.0 nm appear stable, are well aligned with the nanotube axis, and move freely along the nanotube under electron beam irradiation. DWCNTs with inner diameters $d > 1.3$ nm provide increased configurational freedom to carbon chains, causing deviations from axial alignment. Under electron beam irradiation, the as-formed carbon chain radicals may react with defects of the carbon wall and possibly even escape from the confining space of the DWCNTs. Subsequently, they may turn into amorphous carbon covering the DWCNT wall (see the movie in the Supporting Information). We feel positive that this reaction has not been caused by impurities other than carbon, since our electron energy-loss spectra (EELS), presented in Figure S1 of the associated Supporting Information, indicate that only carbon is present in this and all our other samples.

In a second attempt to synthesize diamond nanowires containing only $sp^3$ hybridized carbon, we annealed the ad@DWCNTs samples under hydrogen atmosphere as an alternative to vacuum. This approach should be similar to diamond formation by plasma-enhanced chemical vapor deposition (PE-CVD), which is a free-radical process, in which carbon−carbon bonds form by connecting two carbon-containing radicals, followed by subsequent radical-induced additions, dehydrogenation, and ring closure reactions. In PE-CVD, hydrogen gas is a major reactant and radicals are generated inside a plasma.[38] In higher diamondoid-formation experiments,[23] where reactants were contained in gold tubes, carbon radicals were produced by initial rupture of carbon−carbon bonds. These radicals initiated a chain of reactions, including dehydrogenation and ring closure, that resulted in diamond-cage build-up. Dahl *et al.* also found that carbon radicals containing four carbon atoms (isobutyl radicals) preferentially react with lower

diamondoid reactants promoting growth of higher diamondoids.[23] Under hydrogen atmosphere, no carbon chains were detected in the annealed sample. Absence of vibration modes near 1857 $cm^{-1}$ in the Raman spectra, shown by the red dashed line in Figure 5a, indicates that no carbon chains are present under these conditions. On the other hand, also no diamond nanowires are observed under these conditions. We find no difference between HR-TEM images of the annealed sample (Figure 4b) and the sample prior to annealing (Figure 1d). In view of the high stability of adamantane in a hydrogenating environment,[39,40] we expect that adamantane should remain intact while being annealed inside DWCNTs in hydrogen atmosphere.

In parallel to the experiment, we studied the thermal stability of adamantane molecules inside carbon nanotubes using molecular dynamics (MD) simulations. Since the total time period covered by the MD run was limited to 10 ps, which is very long for *ab initio* simulations yet very short in comparison to the experiment, we artificially increased the temperature to beyond 1200 °C to speed up the dynamics. These simulations have been performed for an infinitely long nanotube, represented by a periodically repeated unit cell containing 168 carbon atoms in the nanotube segment and two $C_{10}H_{16}$ molecules. Alternatively, we investigated the dynamics of two adamantane molecules in a constraining potential modeling the enclosing nanotube and obtained very similar results, which were consistent with our observations.

We analyzed the atomic trajectories by interrogating the atomic pair correlation functions, keeping track of atoms initially associated with each adamantane molecule. Even at temperatures in excess of 1200 °C, we found no indication for an even intermittent detachment of H atoms from adamantane and their recombination to a free $H_2$ molecule. We have also seen no indication that a C−C covalent bond may have been formed intermittently to connect adjacent molecules, or of any atom exchange between adjacent adamantane molecules. We conclude that the adamantane molecules and carbon nanotubes are rather unreactive even at high temperatures if hydrogen is not deliberately removed from the system, further confirming our expectation that adamantane should remain intact in hydrogen atmosphere.

Exploring ways that may yield diamond nanowires, as a working hypothesis, we assumed that such nanowires may form by fusing adamantane molecules and releasing excess hydrogen in molecular form. We calculated the energies of the corresponding reactions with the diamond nanowires of Figure 2b and 2c as final products,

$$7nC_{10}H_{16}(g) \rightarrow 10nC_7H_8\ (\text{nanowire}) + 16nH_2(g) - 10n\cdot\Delta E(C_7H_8) \quad (2)$$

$$4nC_{10}H_{16}(g) \rightarrow 5nC_8H_8\ (\text{nanowire}) + 12nH_2(g) - 5n\cdot\Delta E(C_8H_8) \quad (3)$$

and found both of them to be endothermic, requiring an energy investment between $\Delta E(C_8H_8) = +1.29$ eV and $\Delta E(C_7H_8) = +1.75$ eV per diamond nanowire segment. Consequently, we do not expect a spontaneous formation of diamond nanowires from adamantane molecules encapsulated inside a nanotube.

During thermal annealing of the sample in vacuum, hydrogen atoms were detached from adamantane and dehydrogenated $sp^3$ surface carbon atoms underwent reconstruction to partly hydrogen terminated $sp^2$ nanostructures[41] and ultimately to sp bonded carbon chains. Upon thermal annealing in hydrogen atmosphere, on the other hand, hydrogen detached from the $sp^3$ hybridized carbon was replenished by externally provided hydrogen that prevented further transformation to carbon chain structures.[42,43]

The observed structural changes of linear adamantane assemblies provide a useful indication for ways to change their reaction path to obtain diamond nanowires. The presence of passivating groups is a prerequisite for sustaining $sp^3$ hybridization, which prevents the formation of carbon chains inside carbon nanotubes. To turn the conversion reaction of adamantane molecules exothermic, either the final products have to become more stable, or less stable reactants have to be used. An example of the first scenario contains stable hydrocarbons among the final products, such as

$$nC_{10}H_{16}(g) \rightarrow nC_8H_8\ (\text{nanowire}) + 2nCH_4(g) - n\cdot\Delta E(C_8H_8) \quad (4)$$

which turn the reaction mildly exothermic with $\Delta E(C_8H_8) = -0.46$ eV. Even though this reaction may have occurred under our experimental conditions, we have no indication of forming either $C_8H_8$ nanowires or methane. An example of the second scenario would involve using adamantane derivatives as initial products, which would turn the production of diamond nanowires

$$nC_{14}H_{18}(COOH)_2(g) + 2nH_2(g) \rightarrow 2nC_8H_8\ (\text{nanowire}) + 4nH_2O(g) - n\cdot\Delta E(C_8H_8) \quad (5)$$

also into an exothermic process, with $\Delta E(C_8H_8) = -2.39$ eV.

Finally, we propose an alternative way to convert linear adamantane assemblies to diamond nanowires inside nanotubes in a nonthermal process that would require deposition of large energy amounts, possibly in form of laser pulses or electron beam irradiation.

## CONCLUSIONS

We report the formation of linear arrays of adamantane molecules inside narrow double-wall carbon

nanotubes by a vapor-phase reaction. Our calculations and observations indicate that adamantane encapsulation is highly diameter selective. Whereas no encapsulation was observed in DWCNTs with inner diameters below 0.8 nm, single linear arrays of adamantane molecules assembled inside DWCNTs with inner diameters around 1.0 nm and multiple linear arrays of adamantane were found in DWCNTs with inner diameters exceeding 1.3 nm. The encapsulation of adamantane was confirmed by HR-TEM observations and the shift in the carbon–hydrogen stretch vibration mode of $CH_2$ groups of adamantane molecules from 2897 $cm^{-1}$ in solid adamantane sample to 2917 $cm^{-1}$ in encapsulated adamantane interacting with the nanotube wall.

Our calculations and experimental data indicate that these molecules may selectively react within the narrow confining space inside a carbon nanotube, depending on the surrounding atmosphere and annealing conditions. Upon vacuum annealing above 500 °C, adamantane molecules enclosed in a carbon nanotube have been observed to convert to carbon chains characterized by a sharp Raman feature at 1857 $cm^{-1}$. The intensity of the 1857 $cm^{-1}$ Raman feature, which we interpret as a specific vibration mode of a carbon chain interacting with a nanotube wall, has been demonstrated to be temperature dependent, reaching its maximum at temperatures between 600 and 700 °C. We found that carbon chains in DWCNTs with diameters above 1.3 nm may escape from the enclosing volume of the DWCNTs under electron beam irradiation. In samples annealed at 600 °C in pure hydrogen atmosphere, on the other hand, we found that carbon atoms in adamantane maintained their $sp^3$ hybridization and the adamantane molecules retained their integrity. This result indicates that hydrogen atmosphere is very important for sustaining $sp^3$ hybridized carbon structures.

Our calculation indicate that postulated diamond nanowires with the composition $(C_8H_8)_\infty$ and $(C_7H_8)_\infty$ may fit inside a (7,7) carbon nanotube, but would be significantly less stable than encapsulated adamantane molecules. Their formation would thus require significant energy supply, possibly provided by femtosecond laser pulses, or use of molecules other than adamantane as starting products.

## EXPERIMENTAL METHODS

**Synthesis of Linear Arrays of Adamantane Molecules.** The assembly of linear arrays of adamantane molecules was achieved following the reported vapor phase reaction.[17,44] DWCNTs (Toray Co., 2 mg) were heated at 480 °C for 30 min under air atmosphere to open the caps. The open-ended DWCNTs were degassed at 300 °C for 2 h and then sealed in presence of extra adamantane (Wako, 5 mg) under vacuum of $10^{-6}$ Torr in an H-shaped Pyrex tube. Following sublimation of the adamantane powder, individual molecules were pulled into the void inside DWCNTs by a force resembling the capillary force. The one-dimensional assembly of adamantane molecules was converted to ordered linear adamantane arrays as the sample was heated at 300 °C for 2 days. The as-produced sample was washed by acetone and dried in the oven at 90 °C overnight.

**Thermal Annealing of Linear Adamantane Assemblies.** One part of the as-produced ad@DWCNTs sample was further annealed at temperatures ranging from 450 to 1200 °C for 12 to 48 h under a vacuum of $10^{-7}$ Torr. A second part of the sample was annealed at 600 °C for 12 h, while being flushed by pure hydrogen at a flow rate of 200 sccm.

**Attenuated Total Reflectance Fourier Transform Infrared Spectroscopy (ATR-FTIR).** The samples were first characterized by ATR-FTIR spectroscopy. We used a JASCO FT/IR6100 spectrometer with an attenuated total reflection attachment, JASCO ATR PR410-S. The spectra were obtained with a spectral resolution of 4 $cm^{-1}$ for 1000 scans.

**Raman Spectroscopy.** Raman spectra were taken in a backscattering geometry using a single monochromator with a microscope (HR-800, Horiba Jobin Yvon) equipped with a charge coupled device detector and an edge filter. The samples were excited by argon ions and helium–neon laser wavelengths $\lambda$ = 488, 514, and 633 nm. All measurements were carried out under ambient conditions.

**High-Resolution Transmission Electron Microscopy (HR-TEM).** The structure of the samples was characterized using a JEOL JEM-2100F high-resolution transmission electron microscope that also allowed electron energy-loss spectroscopy (EELS) measurements. The as-produced samples were dispersed in 1,2-dichloroethane using a weak bath sonication technique for 5 min and then dropped onto a thin carbon film suspended on a copper grid. The copper grid was then dried at 100 °C in vacuum ($10^{-6}$ Torr) for 4 h. The HR-TEM images were acquired at an electron acceleration voltage of 80 keV with an exposure time of typically 0.5–1.0 s.

## THEORETICAL METHODS

**Total Energy Calculations.** All structures were optimized using an *ab initio* approach based on the density functional theory (DFT). A judicious choice of the exchange-correlation functional must be made especially in weakly interacting systems such as graphite, where the equilibrium structure determined using the local density approximation (LDA) agrees much better with experiment than that based on the advanced generalized gradient approximation (GGA). Explicit treatment of van der Waals interactions is necessary to obtain precise intermolecular distances at $T = 0$ K in molecular assemblies dominated by these interactions.[45,46] To make static and dynamic simulations of systems with up to 200 atoms manageable, we used the SIESTA code[47,48] with the Ceperley–Alder exchange-correlation functional[49] as parametrized by Perdew and Zunger[50] and described the interaction between valence electrons and ions by norm-conserving pseudopotentials[51] with separable nonlocal operators.[52] Atomic orbitals with double-$\zeta$ polarization were used to expand the electron wave functions with an energy cutoff of 100 Ry or higher for the real-space mesh representation. The confinement energy shift that defines the cutoff radii of the atomic orbitals was set to 0.01 eV. We used periodic boundary conditions for all calculations. Depending on the supercell size, the small Brillouin zone associated with the one-dimensional unit cell was sampled by up to 8 *k*-points in order to properly represent the Bloch wave functions for the momentum–space integration. All geometries have been optimized using the conjugate gradient method,[53]

until none of the residual Hellmann–Feynman forces exceeded $10^{-2}$ eV/Å.

**Molecular Dynamics (MD) Simulations.** Microcanonical and canonical molecular dynamics simulations of free as well as encapsulated diamondoids and their decomposition products inside carbon nanotubes were performed using the SIESTA code. We used the Verlet integration algorithm to cover time periods up to 10 ps with a time step of 0.5 fs.

**Vibration Spectra.** We obtained the vibration spectra of finite fragments and infinite structures by construction the Hessian and the dynamical matrix using the SIESTA code. Alternatively, we obtained the vibration density of states from the velocity–velocity autocorrelation function in MD simulations.

**Model Constraining Potential.** Since it is primarily the shape of the constraining volume and not the chemical character of the carbon nanotube container that directs the assembly and transformation of adamantane molecules, we replaced the surrounding nanotube by a constraining potential of cylindrical symmetry in selected calculations. The constraining potential was determined by extracting pairwise interactions between individual atoms of the enclosed molecule and the surrounding nanotube wall from a large number of *ab initio* calculations for different geometries.

*Conflict of Interest:* The authors declare no competing financial interest.

*Supporting Information Available:* Electron energy loss spectra (EELS) of ad@DWCNT samples, movie of the carbon chains reaction with DWCNTs under electron beam irradiation and movie of the molecular dynamics simulation of adamantane molecules inside a (7,7) nanotube at 1600 °C. This material is available free of charge *via* the Internet at http://pubs.acs.org.

*Acknowledgment.* This work has been supported by Grant-in-Aids for Specific Area Research (No. 19084008) on Carbon Nanotube Nano-Electronics and for Scientific Research A (No. 19205003) of MEXT, Japan, and by the National Science Foundation Cooperative Agreement No. EEC-0832785, titled "NSEC: Center for High-Rate Nanomanufacturing".

## REFERENCES AND NOTES

1. Fokina, N. A.; Tkachenko, B. A.; Dahl, J. E. P.; Carlson, R. M. K.; Fokin, A. A.; Schreiner, P. R. Synthesis of Diamondoid Carboxylic Acids. *Synthesis* **2012**, *44*, 259–264.
2. Schwertfeger, H.; Fokin, A. A.; Schreiner, P. R. Diamonds Are a Chemist's Best Friend: Diamondoid Chemistry beyond Adamantane. *Angew. Chem., Int. Ed.* **2008**, *47*, 1022–1036.
3. McIntosh, G. C.; Yoon, M.; Berber, S.; Tománek, D. Diamond Fragments as Building Blocks of Functional Nanostructures. *Phys. Rev. B* **2004**, *70*, 045401.
4. Ashfold, M. N. R.; May, P. W.; Rego, C. A.; Everitt, N. M. Thin-Film Diamond by Chemical-Vapor-Deposition Methods. *Chem. Soc. Rev.* **1994**, *23*, 21–30.
5. Jing, X; Ma, C.; Ohigashi, Y.; Oliveira, F. A.; Jardetzky, T. S.; Pinto, L. H.; Lamb, R. A. Functional Studies Indicate Amantadine Binds to the Pore of the Influenza A Virus M2 Proton-Selective Ion Channel. *Proc. Natl. Acad. Sci. U.S.A.* **2008**, *105*, 10967–72.
6. Reisberg, B.; Doody, R.; Stöffler, A.; Schmitt, F.; Ferris, S.; Möbius, H. J. Memantine Study Group. Memantine in Moderater-to-Severe Alzheimer's Disease. *New Engl. J. Med.* **2003**, *348*, 1333–41.
7. Dahl, J. E.; Liu, S. G.; Carlson, R. M. K. Isolation and Structure of Higher Diamondoids, Nanometer-Sized Diamond Molecules. *Science* **2003**, *299*, 96–99.
8. Landt, L.; Klünder, K.; Dahl, J. E.; Carlson, R. M. K.; Moeller, T.; Bostedt, C. Optical Response of Diamond Nanocrystals as a Function of Particle Size, Shape, and Symmetry. *Phys. Rev. Lett.* **2009**, *103*, 047402.
9. Yang, W. L.; Fabbri, J. D.; Willey, T. M.; Lee, J. R. I.; Dahl, J. E.; Carlson, R. M. K.; Schreiner, P. R.; Fokin, A. A.; Tkachenko, B. A.; Fokina, N. A.; *et al.* Monochromatic Electron Photoemission from Diamondoid Monolayers. *Science* **2007**, *316*, 1460–1462.
10. Clay, W. A.; Liu, Z.; Yang, W.; Fabbri, J. D.; Dahl, J. E.; Carlson, R. M. K.; Sun, Y.; Schreiner, P. R.; Fokin, A. A.; Tkachenko, B. A.; *et al.* Origin of the Monochromatic Photoemission Peak in Diamondoid Monolayers. *Nano Lett.* **2009**, *9*, 57–61.
11. Clay, W. A.; Sasagawa, T.; Kelly, M.; Dahl, J. E.; Carlson, R. M. K.; Melosh, N.; Shen, Z. X. Diamondoids as Low-Kappa Dielectric Materials. *Appl. Phys. Lett.* **2008**, *93*, 172901.
12. Yao, M.; Stenmark, P.; Abou-Hamad, E.; Nitze, F.; Qin, J.; Goze-Bac, C.; Wågberg, T. Confined Adamantane Molecules Assembled to One Dimension in Carbon Nanotubes. *Carbon* **2011**, *49*, 1159–1166.
13. Smith, B. W.; Monthioux, M.; Luzzi, D. E. Encapsulated $C_{60}$ in Carbon Nanotubes. *Nature* **1998**, *396*, 323–324.
14. Britz, D. A.; Khlobystov, A. N.; Porfyrakis, K.; Ardavan, A.; Briggs, G. A. D. Chemical Reactions Inside Single-Walled Carbon Nano Test-Tubes. *Chem. Commun.* **2005**, 37–39.
15. Smith, B. W.; Luzzi, D. E. Formation Mechanism of Fullerene Peapods and Coaxial Tubes: A Path to Large Scale Synthesis. *Chem. Phys. Lett.* **2000**, *321*, 169–174.
16. Bandow, S.; Takizawa, M.; Hirahara, K.; Yudasaka, M.; Iijima, S. Raman Scattering Study of Double-Wall Carbon Nanotubes Derived from the Chains of Fullerenes in Single-Wall Carbon Nanotubes. *Chem. Phys. Lett.* **2001**, *337*, 48–54.
17. Zhang, J.; Miyata, Y.; Kitaura, R.; Shinohara, H. Preferential Synthesis and Isolation of (6,5) Single-Wall Nanotubes from One-Dimensional $C_{60}$ Coalescence. *Nanoscale* **2011**, *3*, 4190–4194.
18. Schleyer, P. V. A Simple Preparation of Adamantane. *J. Am. Chem. Soc.* **1957**, *79*, 3292–3292.
19. Balaban, A. T.; Schleyer, P. V. Systematic Classification and Nomenclature of Diamond Hydrocarbons. *Tetrahedron* **1978**, *34*, 3599–3609.
20. Lenzke, K.; Landt, L.; Hoener, M.; Thomas, H.; Dahl, J. E.; Liu, S. G.; Carlson, R. M. K.; Möller, T.; Bostedt, C. Experimental Determination of the Ionization Potentials of the First Five Members of the Nanodiamond Series. *J. Chem. Phys.* **2007**, *127*, 084320.
21. Pirali, O.; Vervloet, M.; Dahl, J. E.; Carlson, R. M. K.; Tielens, A. G. G. M.; Oomens, J. Infrared Spectroscopy of Diamondoid Molecules: New Insights into the Presence of Nanodiamonds in the Interstellar Medium. *Astrophys. J.* **2007**, *661*, 919–925.
22. Reiser, J.; McGregor, E.; Jones, J.; Enick, R.; Holder, G. Adamantane and Diamantane; Phase Diagrams, Solubilities, and Rates of Dissolution. *Fluid Phase Equilib.* **1996**, *117*, 160–167.
23. Dahl, J. E. P.; Moldowan, J. M.; Wei, Z.; Lipton, P. A.; Denisevich, P.; Gat, R.; Liu, S.; Schreiner, P. R.; Carlson, R. M. K. Synthesis of Higher Diamondoids and Implications for Their Formation in Petroleum. *Angew. Chem., Int. Ed.* **2010**, *49*, 9881–9885.
24. Han, S.; Yoon, M.; Berber, S.; Park, N.; Osawa, E.; Ihm, J.; Tománek, D. Microscopic Mechanism of Fullerene Fusion. *Phys. Rev. B* **2004**, *70*, 113402.
25. Tommasini, M.; Fazzi, D.; Milani, A.; Del Zoppo, M.; Castiglioni, C.; Zerbi, G. Intramolecular Vibrational Force Fields for Linear Carbon Chains through an Adaptative Linear Scaling Scheme. *J. Phys. Chem. A* **2007**, *111*, 11645–11651.
26. Milani, A.; Tommasini, M.; Fazzi, D.; Castiglioni, C.; Del Zoppo, M.; Zerbi, G. First-Principles Calculation of the Peierls Distortion in an Infinite Linear Carbon Chain: The Contribution of Raman Spectroscopy. *J. Raman Spectrosc.* **2008**, *39*, 164–168.
27. Rinzler, A. G.; Hafner, J. H.; Nikolaev, P.; Lou, L.; Kim, S. G.; Tománek, D.; Nordlander, P.; Colbert, D. T.; Smalley, R. E. Unraveling Nanotubes—Field-Emission from an Atomic Wire. *Science* **1995**, *269*, 1550–1553.
28. Yang, S.; Kertesz, M.; Zolyomi, V.; Kurti, J. Application of a Novel Linear/Exponential Hybrid Force Field Scaling Scheme to the Longitudinal Raman Active Mode of Polyyne. *J. Phys. Chem. A* **2007**, *111*, 2434–2441.
29. Zhao, X. L.; Ando, Y.; Liu, Y.; Jinno, M.; Suzuki, T. Carbon Nanowire Made of a Long Linear Carbon Chain Inserted inside a Multiwalled Carbon Nanotube. *Phys. Rev. Lett.* **2003**, *90*, 187401.

30. Zhao, C.; Kitaura, R.; Hara, H.; Irle, S.; Shinohara, H. Growth of Linear Carbon Chains inside Thin Double-Wall Carbon Nanotubes. *J. Phys. Chem. C* **2011**, *115*, 13166–13170.
31. Jinno, M.; Bandow, S.; Ando, Y. Multiwalled Carbon Nanotubes Produced by Direct Current Arc Discharge in Hydrogen Gas. *Chem. Phys. Lett.* **2004**, *398*, 256–259.
32. Jinno, M.; Ando, Y.; Bandow, S.; Fan, J.; Yudasaka, M.; Iijima, S. Raman Scattering Study for Heat-Treated Carbon Nanotubes: The Origin of Approximate to 1855 $cm^{-1}$ Raman Band. *Chem. Phys. Lett.* **2006**, *418*, 109–114.
33. Fantini, C.; Cruz, E.; Jorio, A.; Terrones, M.; Terrones, H.; Van Lier, G.; Charlier, J. C.; Dresselhaus, M. S.; Saito, R.; Kim, Y. A.; *et al*. Resonance Raman Study of Linear Carbon Chains Formed by the Heat Treatment of Double-Wall Carbon Nanotubes. *Phys. Rev. B* **2006**, *73*, 193408.
34. Nishide, D.; Dohi, H.; Wakabayashi, T.; Nishibori, E.; Aoyagi, S.; Ishida, M.; Kikuchi, S.; Kitaura, R.; Sugai, T.; Sakata, M.; *et al*. Single-Wall Carbon Nanotubes Encaging Linear Chain $C_{10}H_2$ Polyyne Molecules Inside. *Chem. Phys. Lett.* **2006**, *428*, 356–360.
35. Nishide, D.; Wakabayashi, T.; Sugai, T.; Kitaura, R.; Kataura, H.; Achiba, Y.; Shinohara, H. Raman Spectroscopy of Size-Selected Linear Polyyne Molecules $C_{2n}H_2$ ($n$ = 4−6) Encapsulated in Single-Wall Carbon Nanotubes. *J. Phys. Chem. C* **2007**, *111*, 5178–5183.
36. Kazanskii, B. A.; Shokova, E. A.; Korosteleva, T. V. The Pyrolysis of Adamantane. *Izvestiya Akademii Nauk SSSR, Seriya Khimicheskaya* **1968**, *11*, 2640–2642.
37. Ōya, A.; Nakamura, H.; Ōtani, S.; Marsh, H. Carbonization of Adamantane to a Graphitizable Carbon. *Fuel* **1981**, *60*, 667–669.
38. Piekarczyk, W. How and Why CVD Diamond Is Formed: A Solution of the Thermodynamic Paradox. *J. Mater. Sci.* **1998**, *33*, 3443–3453.
39. Aczel, T.; Gorbaty, M. L.; Maa, P. S.; Schlosberg, R. H. Stability of Adamantane to Donor Liquefaction Conditions—Implications toward Structure of Coal. *Fuel* **1975**, *54*, 295–295.
40. Aczel, T.; Gorbaty, M. L.; Maa, P. S.; Schlosberg, R. H. Stability of Adamantane and Its Derivatives to Coal-Liquefaction Conditions, and Its Implications toward the Organic Structure of Coal. *Fuel* **1979**, *58*, 228–230.
41. Barnard, A. S.; Russo, S. P.; Snook, I. K. Structural Relaxation and Relative Stability of Nanodiamond Morphologies. *Diam. Relat. Mater.* **2003**, *12*, 1867–1872.
42. Temelso, B.; Sherrill, C. D.; Merkle, R. C.; Freitas, R. A., Jr. *Ab Initio* Thermochemistry of the Hydrogenation of Hydrocarbon Radicals using Silicon-, Germanium-, Tin-, and Lead-Substituted Methane and Isobutane. *J. Phys. Chem. A* **2007**, *111*, 8677–8688.
43. Hsu, C.-H.; Cloutier, S. G.; Palefsky, S.; Xu, J. Synthesis of Diamond Nanowires Using Atmospheric-Pressure Chemical Vapor Deposition. *Nano Lett.* **2010**, *10*, 3272–3276.
44. Hirahara, K.; Suenaga, K.; Bandow, S.; Kato, H.; Okazaki, T.; Shinohara, H.; Iijima, S. One-Dimensional Metallofullerene Crystal Generated Inside Single-Walled Carbon Nanotubes. *Phys. Rev. Lett.* **2000**, *85*, 5384–5387.
45. Schreiner, P. R.; Chernish, L. V.; Gunchenko, P. A.; Tikhonchuk, E. Y.; Hausmann, H.; Serafin, M.; Schlecht, S.; Dahl, J. E. P.; Carlson, R. M. K.; Fokin, A. A. Overcoming Lability of Extremely Long Alkane Carbon−Carbon Bonds through Dispersion Forces. *Nature* **2011**, *477*, 308–311.
46. Fokin, A. A.; Gerbig, D.; Schreiner, P. R. $\sigma/\sigma$- and $\pi/\pi$-Interactions are Equally Important: Multilayered Graphanes. *J. Am. Chem. Soc.* **2011**, *133*, 20036–20039.
47. Sánchez-Portal, D.; Ordejón, P.; Artacho, E.; Soler, J. M. Density-Functional Method for Very Large Systems with LCAO Basis Sets. *Int. J. Quantum Chem.* **1997**, *65*, 453–461.
48. Soler, J. M.; Artacho, E.; Gale, J. D.; García, A.; Junquera, J.; Ordejón, P.; Sánchez-Portal, D. The SIESTA Method for *ab Initio* Order-*N* Materials Simulation. *J. Phys. Condens. Matter* **2002**, *14*, 2745–2779.
49. Ceperley, D. M.; Alder, B. J. Ground State of the Electron Gas by a Stochastic Method. *Phys. Rev. Lett.* **1980**, *45*, 566–569.
50. Perdew, J. P.; Zunger, A. Self-Interaction Correction to Density-Functional Approximations for Many-Electron Systems. *Phys. Rev. B* **1981**, *23*, 5048–5079.
51. Troullier, N.; Martins, J. L. Efficient Pseudopotentials for Plane-Wave Calculations. *Phys. Rev. B* **1991**, *43*, 1993–2006.
52. Kleinman, L.; Bylander, D. M. Efficacious Form for Model Pseudopotentials. *Phys. Rev. Lett.* **1982**, *48*, 1425–1428.
53. Hestenes, M. R.; Stiefel, E. Methods of Conjugate Gradients for Solving Linear Systems. *J. Res. Natl. Bur. Stand.* **1952**, *49*, 409–436.